Available online at www.sciencedirect.com
SCIENCE DIRECT®
Catalysis Today 89 (2004) 143–150
CATALYSIS TODAY
www.elsevier.com/locate/cattod

Combination of low and high temperature catalytic materials to obtain broad temperature coverage for plasma-facilitated NO_x reduction

K.G. Rappé[a,*], J.W. Hoard[b], C.L. Aardahl[a], P.W. Park[c], C.H.F. Peden[a], D.N. Tran[a]

[a] *Pacific Northwest National Laboratory, Box 999 MS K6-28, Richland, WA 99352, USA*
[b] *Ford Research Laboratory, P.O. Box 2053, MD 3179 SRL, Dearborn, MI 48121, USA*
[c] *Caterpillar Inc., Tech Center E/854, P.O. Box 1875, Peoria, IL 61656, USA*

Abstract

Two catalysts, Ba/zeolite Y and Ag/γ-alumina, were combined to reduce NO_x in simulated lean exhaust using plasma-facilitated catalysis. Steady-state experiments conducted at 473, 623, and 773 K show that ordering of the catalysts impacts NO_x conversion, and maximum efficiency is obtained when the zeolite material precedes the alumina. Optimal ordering results in greater than 80% conversion at 473 K, and efficiencies greater than 95% were obtained at 623 and 773 K under steady operation when propene was added as a reductant at C_1:NO_x = 12. Temperature cycling experiments covering the temperature range 373–773 K were used to determine a 'transient' cycle efficiency of 70% for the optimal catalyst configuration. Results of these experiments suggest that preferred ordering likely results in better management of stored NO_x when transients to higher temperature occur. Studies also show that improved hydrocarbon utilization is evident in the optimal configuration due to the nature of the partially oxidized hydrocarbons that are formed at various stages of during the plasma-facilitated catalytic NO_x reduction process.

Keywords: NO_x reduction; Non-thermal plasma; Hydrocarbons; Silver-alumina; Barium-zeolite Y

1. Introduction

Diesel engines are attractive because their lean burn operation result in high fuel economy. The wear characteristics and ability to deliver power efficiently under high load conditions are also noteworthy advantages of diesel propulsion. Potential reduction in consumption of fossil fuels and reduction in greenhouse gas emissions could be achieved if greater diesel penetration were possible in the marketplace. However, advancement of diesel market share in future years will be limited unless engine emissions issues can be resolved. The high thermal efficiency of diesel engines is burdened with particulate matter (PM) and nitrogen oxides (NO_x) emissions that exceed levels mandated by the United States Environmental Protection Agency (US EPA) starting in 2007 and phasing in completely by 2010 [1,2]. Tier II limits for on road heavy-duty vehicles will be imposed for commercial vehicles such as long haul trucks and city buses as well as light-duty vehicles such as light trucks and smaller personal vehicles. It is expected that PM emissions will be addressed by the use of particulate filtration technology currently in advanced development [3], but reduction of NO_x emissions remains a difficult barrier. For example, any NO_x reduction approach for on highway trucks must reduce emissions by 90–95% from 2002 levels to reach the 2010 target.

In the late 1980s, the concept of active lean NO_x catalysis was introduced, where hydrocarbons are used as a reducing agent to assist NO_x reduction to N_2 over a suitable catalyst [4,5]. Since that time, promising NO_x abatement technologies have been examined, but each of these technologies has limitations. NO_x-adsorber catalysis, so-called lean NO_x traps (LNTs), is an advancement of the well-established three-way catalyst technology used in gasoline-powered vehicles [3], but it suffers under even limited sulfur exposure. Recent results show that sulfur-poisoned LNTs can be regenerated against sulfur poisoning using high temperature excursions that result in desulfation of the catalyst surface [6,7]. However, LNTs remain quite expensive for broad market acceptance due to high precious metal loading [8]. Another potential NO_x emission control strategy is selective catalytic reduction (SCR) of NO_x with urea [3]. Certain bins in the EPA Tier II regulations for 2007 have

* Corresponding author.

0920-5861/$ – see front matter © 2003 Elsevier B.V. All rights reserved.
doi:10.1016/j.cattod.2003.11.020

been met with this approach [9]. However, the logistics of wide-scale distribution of urea is a significant concern for implementation in the time frame required.

Plasma-facilitated, lean NO_x catalysis (PFC) using hydrocarbon reducing agents is another technology receiving limited attention for the reduction of NO_x in light and heavy-duty applications [10–18]. Plasma-facilitated catalysis is a two-step process consisting of plasma pretreatment of the exhaust before flow over a lean NO_x catalyst. Hydrocarbon is added to the exhaust to enable specific oxidation chemistry in the plasma and subsequent NO_x reduction chemistry over the catalyst. Oxidation of NO to NO_2 takes place in the first step. Although this is not a required characteristic on some catalysts, it does transform NO_x to the more reactive NO_2 form, which has been demonstrated to enhance activity at lower temperatures due to the higher reactivity of the NO_2 versus NO. In the second stage, NO_x is converted to N_2 over the catalyst while hydrocarbons are consumed. The plasma also partially oxidizes hydrocarbon, which is now recognized to be a source of critical intermediates for NO_x reduction [19–25]. Another secondary benefit of the plasma is the oxidation NO and hydrocarbons without oxidizing SO_2 to SO_3, which allows a broad range of catalysts to be more resistant to typical aging concerns [26].

Using experiments and simulation, Penetrante et al. [19,27] conducted extensive studies on the gas phase chemistry in the plasma oxidation step. Findings indicated that plasma treatment of lean exhaust alone does not lead to formation of NO_2. In the absence of added hydrocarbon, $O^{\bullet}$ is formed and converts NO_2 back to NO in simulated lean exhaust. Hydrocarbon serves as an $O^{\bullet}$ sink, and byproducts of the $O^{\bullet}$ consumption process include peroxyl radicals ($RO_2^{\bullet}$, $HO_2^{\bullet}$). Peroxyl radicals allow conversion of NO to NO_2 without back reactions taking place [19,20]. The second step in PFC involves active lean NO_x catalysis, primarily with NO_2 and partially oxidized hydrocarbons. As noted above, plasma treatment of exhaust gases results in some degree of partial oxidation of the hydrocarbon reducing agent. Recent studies have shown that the nature of the hydrocarbon species can have a large impact on the thermal catalytic and plasma catalytic performance of lean NO_x catalysts, and oxygenates in particular appear to be critical intermediates over many catalytic materials [19–25,28].

Several investigations have shown that the addition of alkali and alkaline earth species (for zeolites) or transition metal ions (for γ-alumina) enhances catalytic activity [29–43]. Metals activate hydrocarbons and may provide sites for conversion of NO_x and hydrocarbons to surface intermediates like organonitrile, isocynate, or formate species [29,30,38–45]. Therefore, when plasma pretreatment of exhaust is combined with metal-promoted catalysis, there is an opportunity to take advantage of hydrocarbon activation through the plasma and over promoter sites on the catalyst. Recent PFC results on in-promoted γ-alumina catalysts demonstrated that these two activation mechanisms must be balanced to maximize conversion [28].

Many catalyst formulations have been proposed and tested for lean NO_x activity. For lower exhaust temperatures (<550 K), Cu/ZSM-5 has shown interesting results, but CuZSM-5 shows low durability at higher exhaust temperatures [46–48]. In plasma operation, best success at low temperatures (423–543 K) has been achieved using catalysts based on zeolite Y supports [22]. For higher temperatures (>573 K) catalysts based on γ-alumina have shown the most promise because of their durability at higher temperatures and high thermal activity, particularly when reaction temperatures approach 673 K.

The temperature ranges for light-duty and heavy-duty diesel exhaust overlap in the 473–623 K range. In general, the zeolite Y catalysts do not deliver appreciable activity at the high end of the light-duty range, and the γ-alumina catalysts are insufficient at the low end of the heavy-duty range. The overlap in the activity ranges occurs where NO_x reduction activity transitions from zeolite Y to γ-alumina materials. Therefore, it is not surprising that mixtures of catalysts have been used to broaden the active temperature window for both light-duty and heavy-duty applications. The first report of such an approach was made by Panov et al. [22], and other reports have followed more recently [49]. In this paper, the catalyst combination Ba/zeolite Y and Ag/γ-alumina is examined under steady and transient operation.

2. Experimental

2.1. Catalyst preparation

The Ag/γ-alumina catalyst tested under 'steady-state' conditions was doped with 0.95 wt.% Ag on γ-Al_2O_3. The γ-Al_2O_3 support (Puralox, Condea Vista) had a BET surface area of 145 m^2/g, pore volume of 1.08 mL/g, and particle size distribution as follows: 44.1% <25 μm, 75.0% <45 μm, and 99.3% <90 μm. Silver impregnation was achieved using the incipient wetness technique with a solution of $AgNO_3$. The impregnated samples were dried in air at 373 K for 24 h and calcined by ramping at 30 K/h to 1023 K, holding for 30 min, and ramping down at 300 K/h.

The γ-alumina support [surface area 230 m^2/g, pore volume 1 ml/g, particle size of 5 nm wide and 20 nm long (from TEM image)] used in the 'transient' experiments was prepared by a sol–gel method using alumina isopropoxide and 2-methyl-2,4-pentanediol as a complexing agent. The procedure for the alumina preparation has been described previously [50]. A 4 wt.% Ag/Al_2O_3 catalyst was prepared using the incipient wetness technique with γ-alumina powder and an aqueous solution of silver nitrate. Here, higher silver loading on the catalyst was better for the higher sulfur levels used in the 'transient' test conditions described below. The impregnated samples were dried in air at 373 K for 24 h and calcined at temperatures up to 873 K (ramp rate: 1.2 K/min) for 5 h under flowing air at 5 SLM.

The barium/zeolite Y (BaZY) catalyst used in the 'steady-state' and 'transient' experiments was prepared via solution ion exchange of Ba^{2+} on sodium/zeolite Y (NaZY) powder (CBV100, Zeolyst International). A $Ba(NO_3)_2$ aqueous solution was mixed with NaZY powder at a ratio of 0.614 g Ba per gram NaZY powder. The resultant product was centrifuged, decanted, recovered, and a second $Ba(NO_3)_2$ aqueous solution added. When complete, that product was recovered in the same manner (with additional rinsing with DI water and centrifuging) and dried in a vestibule in a drying oven at 323 K for 1–2 h. The product was then calcined at 773 K for 2 h at a thermal ramp of 10 K/min.

2.2. 'Steady-state' testing (Pacific Northwest National Laboratory)

A feed gas consisting of 500 ppm NO, 300 ppm CO, 8% CO_2, 1.5% H_2O, 2 ppm SO_2, 9% O_2, 2000 ppm C_3H_6, and balance of N_2 was used for the steady-state testing. NO, CO, CO_2, SO_2, O_2, and hydrocarbon were mixed together as dry gases and combined with a humid N_2 stream to achieve 1 L/min total simulated exhaust. Gases are mixed and carried to the PFC system using room temperature PTFE lines. The humidified stream is sent to a two-stage high-temperature apparatus consisting of a pair of tubular furnaces. The first furnace housed a high-temperature plasma reactor, and the second furnace housed the catalysts of interest.

The apparatus employed for steady-state measurements is shown in Fig. 1. Three gas sampling locations were used: pre-plasma, post-plasma, and post-catalyst. The sample ports were connected to a three-position valve, which routed the entire flow through a nafion-tube diffusion dryer (Mini-GASS, Perma Pure, Inc.) prior to transfer to the analytical systems. Analytical capabilities included a Rosemount 951A Chemiluminescence NO/NO_x Analyzer and a Nicolet 210 FTIR spectrometer with a 10 m path length for measurement of IR active species. Measurements shown here were acquired with the chemiluminescence analyzer, and FTIR measurements were used to show accurate calibration of the analyzer.

The concentric cylinder plasma reactor was the first stage of the apparatus. The reactor was formed using a 12.5 mm OD alumina tube inside of a 25 mm OD alumina tube. A section of the 12.5 mm tube was packed with stainless steel wool, forming the high-voltage electrode, and the corresponding section of the 25 mm tube was sheathed by stainless steel mesh, forming the ground electrode. A non-thermal dielectric discharge was formed in the annulus between the two tubes. 1 L/min of simulated exhaust stream flowed through this region at a space velocity of $\sim$4000 h^{-1}. The high-voltage electrode was electrified using 3–9 kV(rms) from a Corona Magnetics high voltage transformer. The transformer was powered by an audio amplifier (RMX1450, QSC), which in turn was driven by a waveform generator (3011B, BK Precision). Typical operating frequency was in the range of 100–400 Hz. A 1000:1 high-voltage probe monitored the voltage supplied to the high-voltage electrode, and the ground current was sent through a 2 μF capacitor to monitor the plasma discharge current. After conditioning, these two signals are monitored by a Lecroy 9420 dual oscilloscope and power is calculated via a Visual Basic program that determines the area of the voltage versus current curve acquired from the oscilloscope [51]. Energy density deposited in the gas ranged from 0 to 150 J/L. A catalytic reactor made up the second stage of the apparatus. The reactor consisted of a 25 mm OD quartz tube with a bed of catalyst powder held in place by quartz wool. Typical catalyst loadings were 1–2 g. Space velocities ranged from 14,000 to 29,000 h^{-1}, depending on test configuration and bulk density of the powders used.

The temperature of each stage was controlled independently via the tube furnaces housing each reactor. Each catalyst configuration was examined at 473, 623, and 773 K, with the plasma and catalyst reactors held at the same temperature. This allowed plasma-assisted catalyst activity to be examined over the range of interest for heavy-duty diesel exhaust, representing idle, road, and high-load conditions

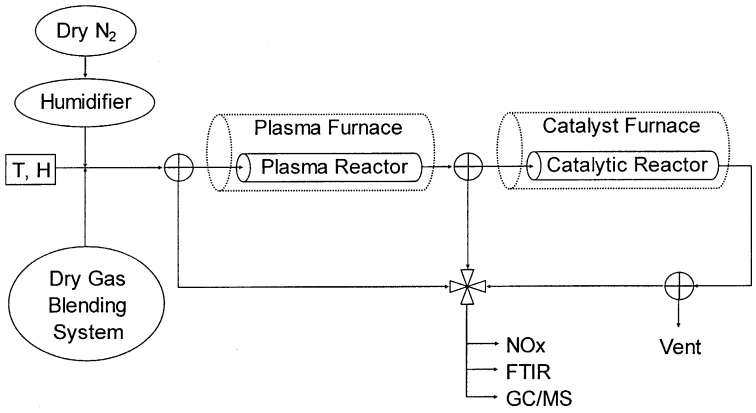

Fig. 1. Schematic of the exhaust treatment test stand used for steady-state PFC measurements.

for the engine. The low end of this range also represents conditions of interest for light-duty applications.

2.3. 'Transient' testing (Ford Research Laboratories)

The experimental set-up and furnace apparatus described below is based on the same principles as the apparatus used for steady-state testing. A feed gas composed of 260 ppm NO, 5 ppm NO_2, 0 or 50 ppm SO_2, 7% CO_2, 7% O_2, 1% Ar, 400 ppm CO, 133 ppm H_2, 500 ppm C_3H_6, 133 ppm C_3H_8, 2.8% H_2O, and a balance of N_2 was used for the transient tests. The dry gases were mixed and passed over a heated wick, where water was added, thereby humidifying the gas while avoiding pulsation effects due to direct pumping. The resulting humidified gas was fed via heated stainless steel lines to a test stand consisting of two ovens in series.

The first oven housed a parallel-plate dielectric-barrier discharge device with embedded electrodes, operated at a space velocity of 150,000 h^{-1}. The reactor was powered by a Trek Model 10/10, driven by a HP 33120A function generator. Power was measured using a Tektronix TDS420A oscilloscope that received signals from a Tektronix P6015A high-voltage probe and a 1 kΩ current sense resistor in series with the reactor. Power was held constant at 30 J/L via a Labview program running a PID control algorithm, where power regulation is adjusted by changes in AC frequency. The second oven housed a 25 mm quartz tube containing the catalyst(s) of interest. Typical space velocity in the catalyst was 12,000–20,000 h^{-1}. Both ovens were equipped with cooling air and were programmable for thermal cycling.

The 4 L/min flow of test gas was diluted 5:1 with nitrogen following the second oven to avoid water condensation at room temperature, resulting in 20 L/min through the analytical instruments. Primary analyses for NO_x were performed with a Mattson Nova Cygni 120 Fourier Transform Infrared (FTIR) Analyzer (0.25 wavenumber resolution) equipped with a Foxboro 21.75 m gas cell. Conventional Horiba emission analyzers included IR for CO and CO_2, flame ionization for total hydrocarbons, magneto-pneumatic for O_2.

Thermal cycling was performed between 373 and 773 K with a ramp rate of 10 K/min. At each end of the ramp, the minimum or maximum temperature was held for 12 min prior to heating or cooling, respectively. For all transient results reported herein, the data shown are for the final cycle on the material. The final cycle was determined by waiting until two consecutive cycles overlapped, which typically occurred in 3–4 loops. Taking the data during consistent loops insured that the material had reached a quasi-steady condition where loading and desorption of the catalyst over the cycle occurred to the same extent. We should stress that the transient cycling used here does not correspond to any known transient testing protocols; its only function is to understand how the material behaves during thermal cycling.

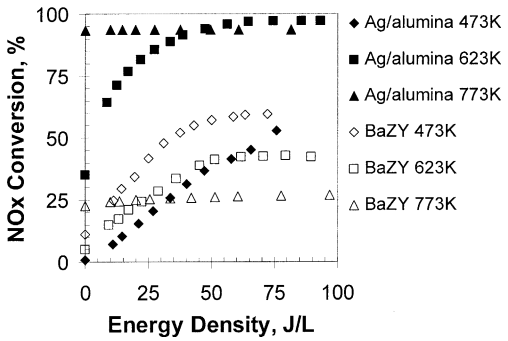

Fig. 2. Steady-state performance of individual catalysts: 0.95 wt.% Ag/Al_2O_3 and BaZY. The 'steady-state' gas mixture at a flow rate of 1 SLM was used with 1 g of catalyst.

3. Results and discussion

3.1. Individual catalysts

The BaZY catalyst and Ag/Al_2O_3 catalyst were tested independently using 1 g of catalyst and the steady-state test mixture with propene as the reducing agent. Fig. 2 shows these isothermal test results at 473, 623, and 773 K. The shapes of the curves are typical for PFC data sets. Typically, lower temperature data show a sharp rise in conversion as specific energy deposition increases, which is a result of formation of oxygenated hydrocarbons and NO_2 in the plasma leading to higher conversion rates over the catalyst. At high temperature, the plasma does not show benefit due to the high thermal activity of the catalyst. From Fig. 2, BaZY demonstrates consistently higher activity than Ag/Al_2O_3 at 473 K, with roughly double the activity at ∼50 J/L. With higher temperatures the BaZY activity dropped, whereas the Ag/Al_2O_3 catalyst demonstrates significantly higher activity, reaching 97% NO_x conversion at 623 K and 94% conversion at 773 K, in comparison to 43 and 27% for the BaZY, respectively. This is an expected result based on previous investigation of each of these materials. Panov et al. [22] showed BaZY catalyst activity over the temperature range of 423–573 K, with conversion decreasing significantly at higher temperatures. Alumina-based catalysts have been studied extensively for higher temperature operation. Doping of the catalyst with Ag leads to better activity at lower temperatures (623 K) than γ-alumina itself. However, hydrocarbon consumption becomes a significant factor at 773 K due to activation by the silver sites, which is believed to be the reason greater NO_x conversion is achieved at 623 K compared to 773 K.

Results from transient testing on BaZY are shown in Fig. 3. Here, 6 g of catalyst were used. Arrows indicate the direction of the loop for the temperature transient. The data in Fig. 3 confirm that BaZY activity peaks at 473 K and decreases at higher temperatures. An important feature here is the hump observed in NO and NO_2 levels around 423 K. Such behavior indicates NO_x storage on the catalyst at lower temperatures. Cycling up in temperature results in thermal

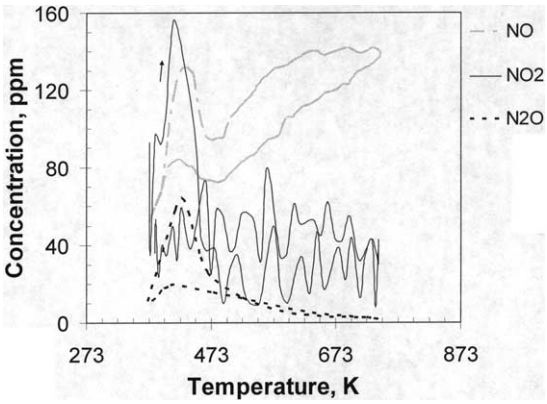

Fig. 3. Effluent NO_x species after PFC treatment with BaZY catalyst. The 'transient' gas mixture at a flow rate of 4 SLM was used with 6 g catalyst. Arrows indicate the direction of increasing temperature in the 'transient' loop.

desorption and a resulting increase in NO_x levels. The data also indicate that in the active temperature regime some N_2O is formed over BaZY, which is consistent with prior reports [21].

Results from transient testing on Ag/Al_2O_3 are shown in Fig. 4. Again, 6 g of catalyst was used. There is no evidence of N_2O formation on this catalyst, and the NO_x traces have many features seen in the BaZY data. Storage of NO is greater on this catalyst than for BaZY, and the affinity for NO to the surface is slightly higher, which is indicated by the shift in desorption peak to somewhat higher temperature. The NO_2 storage is subtle and does not display a sharp peak as in the BaZY case. Variations in the NO_2 levels result from noise in the data caused by the difficulty of automatic analysis of FTIR data when several species are present. Negative values in concentration result from dips below the zero level relative to baseline spectra. Where oscillations are observed in concentration, a smoothed or average value is representative of the actual NO_x concentration. NO_x levels on the

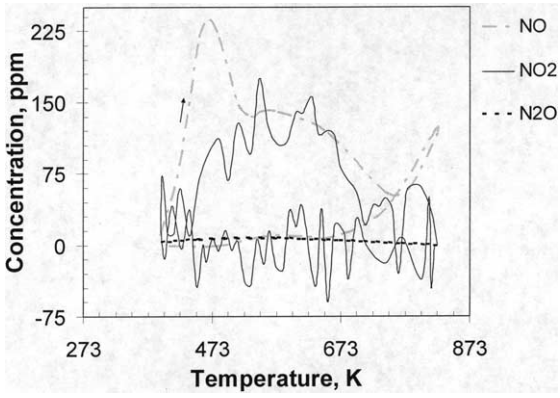

Fig. 4. Effluent NO_x species after PFC treatment with Ag/Al_2O_3 catalyst. The 'transient' gas mixture at a flow rate of 4 SLM was used with 6 g catalyst. Arrows indicate the direction of increasing temperature in the 'transient' loop.

Ag/Al_2O_3 drop precipitously above 573 K with maximum conversion occurring at ~748 K. Above this temperature hydrocarbon combustion over the catalyst starts to dominate and limits availability of reductants for NO_x conversion.

3.2. Catalyst mixtures

Fig. 5 shows the test results where BaZY and Ag/Al_2O_3 were tested together under 'steady-state' reaction conditions. Three testing configurations were examined: (i) powders completely mixed, (ii) Ag/Al_2O_3 followed by BaZY, and (iii) BaZY followed by Ag/Al_2O_3. In each case the 2 g catalyst bed was composed of equal weights of each catalyst, and all data were taken at 50 J/L. It is clear from examination of the data that proper staging of the catalysts is critical to obtaining maximum conversion. In particular, configuration (iii) shows consistently higher NO_x conversion results for all temperatures examined. Over 95% efficiency at 623 and 773 K, and over 80% conversion at 473 K were obtained. This is an important result in that such high NO_x conversion efficiencies have not been previously demonstrated over such a wide range of temperature.

Comparison of these data to the results obtained with the individual catalysts is not straightforward because of the different amounts of catalyst used. The space velocity was held constant in each of the experiments for a given catalyst, but in the dual catalyst experiments the overall space velocity is half that of the single catalyst experiments. Activity over a broader temperature range is certainly evident; therefore, it seems as though the specific desirable characteristics of each catalyst contribute to overall reactivity in their respective temperature regimes. However, the reason for improved performance when the catalysts are sequenced with BaZY before Ag/Al_2O_3 cannot be understood from the NO_x conversion data alone. In order to better understand why this specific catalyst ordering is important, NO_x reduc-

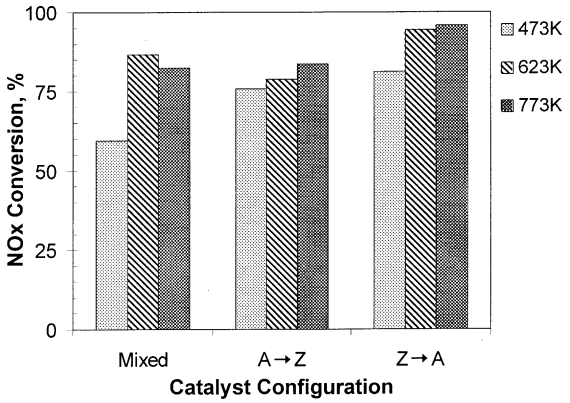

Fig. 5. 'Steady-state' NO_x conversion for three cases where mixed catalysts were used. "Mixed" indicates a homogeneous mixture of powders. A → Z indicates alumina preceding zeolite, and Z → A indicates zeolite preceding alumina. In all cases, a 'steady-state' gas mixture at a flow rate of 1 SLM was used. Each catalyst of 1 g of (2 g total) was loaded into the reactor for these tests.

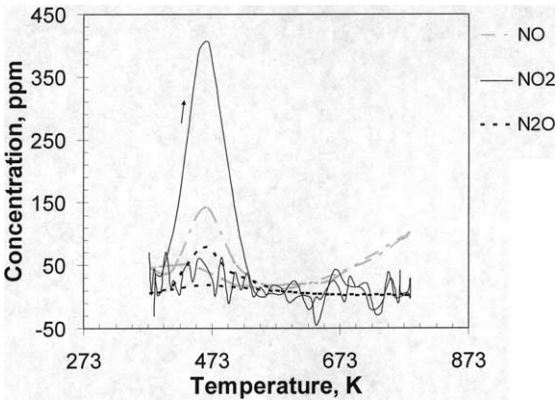

Fig. 6. Effluent NO_x species after PFC treatment with the Z → A catalyst configuration. The 'transient' gas mixture at a flow rate of 4 SLM was used with 6 g BaZY followed by 3 g Ag/Al_2O_3. Arrows indicate the direction of increasing temperature in the 'transient' loop.

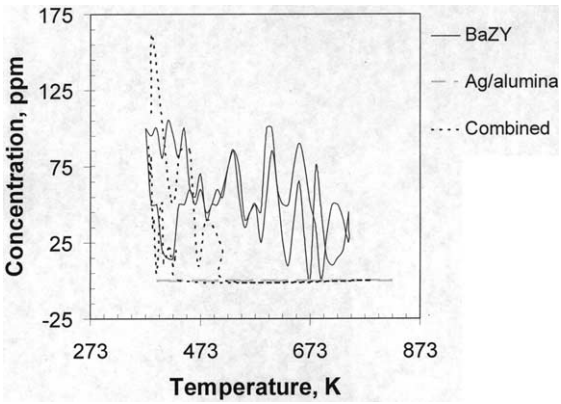

Fig. 7. Acetaldehyde levels observed in transient testing with individual catalysts and the optimal configuration.

tion performance and the speciation of the hydrocarbons were examined using 'transient' experiments.

Fig. 6 shows effluent NO_x concentrations from the optimal dual catalyst system under transient conditions. Here, 6 g of BaZY preceded 3 g of Ag/Al_2O_3. The data show that low temperature storage is still a concern; however, overall NO_x levels are lower when compared to the single catalysts, and the temperature where maximum efficiency is observed (~573 K) shifts to the point where the activity of both catalysts overlap substantially. Also of interest is the larger NO_2 desorption peak; in fact, compared to the single catalyst data, the amount of adsorbed NO_2 increases substantially. It is possible that intermediates formed on the BaZY allow more efficient storage of NO_2 on Ag/Al_2O_3. This is supported by the data in Fig. 3 that show the predominant form of NO_x discharged from BaZY is NO_2 at low temperature. The fact that the mean desorption temperature for NO_2 on the dual catalyst configuration is near 473 K also supports the theory of NO_2 storage on Ag/Al_2O_3 at low temperature because that desorption temperature is consistent with what was observed on the Ag/Al_2O_3 alone. It is also conceivable that NO_x stores on the zeolite and a portion is desorbed and shifted to the alumina as the temperature increases between 423 and 473 K.

Additional information on the dual catalyst system can be obtained by following the fate of the partially oxidized hydrocarbon intermediates that are formed in the plasma reactor over each of the catalysts alone and in their optimum dual catalyst configuration. Figs. 7 and 8 show the acetaldehyde and formaldehyde levels, respectively, for each of the cases. Fig. 7 shows that there are no appreciable acetaldehyde levels following the Ag/Al_2O_3 alone. However, in both cases where the BaZY is present, noticeable levels of acetaldehyde exit the reactor. For BaZY alone, acetaldehyde utilization increases slightly as temperature increases. For the Z → A dual catalyst configuration, acetaldehyde levels fall to zero at temperatures above 473 K.

Fig. 8 shows that formaldehyde levels actually increase over the temperature range examined following a BaZY catalyst alone. This is consistent with previous reports by Panov et al. [52] who showed that formaldehyde is inactive for NO_x reduction over BaZY. In fact, the increasing levels indicate that formaldehyde is formed over the BaZY catalyst at higher temperatures. As also seen for acetaldehyde, formaldehyde is consumed to nearly completion following the dual catalyst formulation indicating that Ag/Al_2O_3 utilizes both of these species to accomplish NO_x reduction. Thomas et al. [24] showed that formaldehyde was an excellent reducing agent for use with Ag/Al_2O_3, so it is reasonable to assume that production of formaldehyde by BaZY is the critical aspect that makes this particular configuration perform so well for NO_x reduction. An added benefit of the configuration is the lower hydrocarbon slip due to high utilization of the hydrocarbon.

3.3. NO_x efficiency of the optimal configuration

Fig. 5 shows the NO_x efficiency under 'steady-state' reaction conditions. This represents the highest activity ever reported over such a broad temperature range. The perfor-

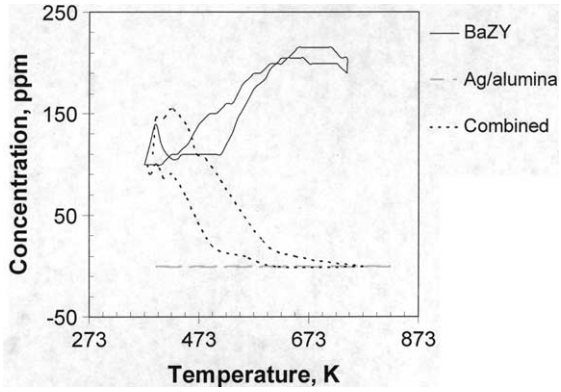

Fig. 8. Formaldehyde levels observed in transient testing with individual catalysts and the optimal configuration.

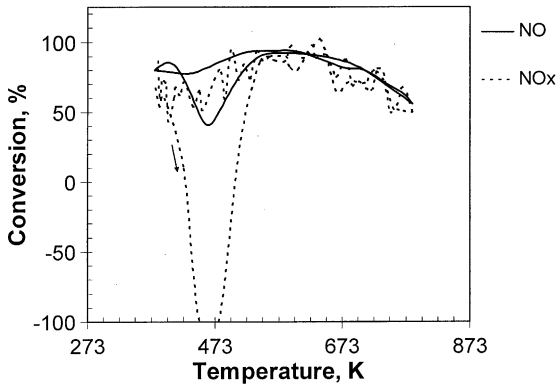

Fig. 9. 'Transient' NO_x conversion for the Z → A configuration. The 'transient' gas mixture at a flow rate of 4 SLM was used with 6 g BaZY followed by 3 g Ag/Al_2O_3. Arrows indicate the direction of increasing temperature in the 'transient' loop.

mance under 'transient' conditions is also of interest. Fig. 9 shows the NO_x conversion plot for the 'transient' case. For most of the cycle the conversion is quite high at 60–95%; however, the desorption of NO_2 on the heating ramp from low temperature detracts significantly from the overall NO_x conversion for a cycle. Even with the large degree of NO_2 desorption, the overall NO_x reduction for the cycle is still around 70%. This represents the highest level reported in such an experiment, and a significantly higher level than in the single catalyst cases examined here. It is plausible that management of the hydrocarbon levels (e.g., inject more hydrocarbon during engine load increases) during realistic vehicle exhaust temperature transients could result in better control of overall NO_x conversion, especially by reducing the deleterious effects of NO_x desorption during temperature spikes.

4. Conclusions

Placing BaZY upstream of Ag/Al_2O_3 enhanced the NO_x reduction activity over the BaZY or Ag/Al_2O_3 catalysts used individually. Data reported here support the explanation that higher activity is due to significant formation of formaldehyde over BaZY that can be effectively used as a reducing agent over Ag/Al_2O_3. Under steady operation conversion ranged from 80 to in excess of 95%, and under 'transient' operation a cycle average of 70% reduction was achieved. The drop in efficiency in cycled operation is attributed to NO_x desorption during heating 'transients' below 473 K. However, it seems reasonable to suggest that the optimal configuration will be especially beneficial during realistic temperature transients due to the fact that during NO_x desorption, the downstream catalyst may be reaching temperatures where it is active, resulting in partial conversion of the desorbed NO_x. It may also be possible to control the hydrocarbon levels in a manner that alleviates the pulses of NO_x that evolve during catalyst heating.

Acknowledgements

This research was performed in part using the Interfacial and Nanoscale Science Facility (INSF) in the William R. Wiley Environmental Molecular Sciences Laboratory, a national scientific user facility sponsored by the US Department of Energy's Office of Biological and Environmental Research and located at the Pacific Northwest National Laboratory.

This work was funded under two Cooperative Research and Development Agreements, one between Pacific Northwest National Laboratory and Caterpillar Inc. and the other between Pacific Northwest National Laboratory and the Low Emission Technologies Research and Development Partnership. The authors are grateful to the US Department of Energy, Office of FreedomCAR & Vehicle Technologies for supporting this program. Pacific Northwest National Laboratory is operated by Battelle for the US Department of Energy under Contract DE-AC06-76RLO 1830.

References

[1] US Environmental Protection Agency, Office of Transportation and Air Quality, Regulatory Announcement: Heavy-Duty Engine and Vehicle Standards and Highway Diesel Fuel Sulfur Control Requirements. EPA420-F-00-057, December 2000.
[2] C. Shenk, C. Laroo, SAE Technical Paper Series #2003-01-0042, SAE, Warrendale, PA, 2003.
[3] US Environmental Protection Agency, Office of Transportation and Air Quality, Heavy-Duty Standards/Diesel Fuel RIA: Emission Standards Feasibility, EPA420-R-00-026, December 2000, Chapter III.
[4] W. Held, A. Koenig, German Offen. DE 3,642,018 (1987).
[5] Y. Fujitani, H. Muraki, A. Nagoya, S. Kondoh, M. Fukui, A. Toyoake, German Offen. DE 3,735,151 (1988).
[6] J. Parks, B. Epling, A. Watson, G. Campbell, Durability of NO_x adsorbers, in: Presentation Given at the Eighth Diesel Engine Emissions Reduction Conference, US DOE FreedomCAR and Vehicle Technologies, San Diego, CA, August 25–29, 2002.
[7] T.V. Johnson, SAE Technical Paper Series #2003-01-0039, SAE, Warrendale, PA, 2003.
[8] S. Faulkner, NO_x adsorber development, in: Presentation Given at the Eighth Diesel Engine Emissions Reduction Conference, US DOE FreedomCAR and Vehicle Technologies, San Diego, CA, August 25–29, 2002.
[9] R. Hammerle, Urea Selective Catalytic Reduction and Diesel Particulate Filter System for Diesel Sport Utility Vehicle Meeting Tier II Bin 5, in: Presentation Given at the Eighth Diesel Engine Emissions Reduction Conference, US DOE FreedomCAR and Vehicle Technologies, San Diego, CA, August 25–29, 2002.
[10] J. Hoard, H. Servati (Eds.), Plasma Exhaust After Treatment, SAE SP-1395, SAE, Warrendale, PA, 1998.
[11] M.L. Balmer, G. Fisher, J. Hoard (Eds.), Non-thermal plasma for exhaust emission control: NO_x, HC, and particulates, SAE SP-1483, SAE, Warrendale, PA, 1999.
[12] M.L. Balmer, G. Fisher, J. Hoard (Eds.), Non-thermal plasma, SAE SP-1566, SAE, Warrendale, PA, 1998.
[13] M.L. Balmer, G. Fisher, J. Hoard (Eds.), Non-thermal plasma emission control systems, SAE SP-1639, SAE, Warrendale, PA, 1998.
[14] S. Yoon, A.G. Panov, R.G. Tonkyn, A.C. Ebeling, S.E. Barlow, M.L. Balmer, Catal. Today 72 (2002) 243.

[15] S. Yoon, A.G. Panov, R.G. Tonkyn, A.C. Ebeling, S.E. Barlow, M.L. Balmer, Catal. Today 72 (2002) 251.
[16] L.-Q. Wang, C.L. Aardahl, K.G. Rappe, D.N. Tran, M.A. Delgado, C.F. Habeger, J. Mater. Res. 17 (2002) 1843.
[17] J. Hoard, SAE Technical Paper Series #2001-01-0185, SAE, Warrendale, PA, 2001.
[18] C.L. Aardahl, K.G. Rappe, P.W. Park, C.S. Ragle, C.L. Boyer, S.A. Faulkner, SAE Technical Paper Series #2003-01-1186, SAE, Warrendale, PA, 2003.
[19] B.M. Penetrante, R.M. Brusasco, B.T. Merrit, W.J. Pitz, G.E. Vogtlin, M.C. Kung, H.H. Kung, C.Z. Wan, K.E. Voss, SAE Technical Paper Series #982508, SAE, Warrendale, PA, 1998.
[20] R. Dorai, M.J. Kushner, SAE Technical Paper Series #1999-01-3683, SAE, Warrendale, PA, 1999.
[21] J.W. Hoard, A. Panov, SAE Technical Paper Series #2001-01-3512, SAE, Warrendale, PA, 2001.
[22] A.G. Panov, R.G. Tonkyn, M.L. Balmer, C.H.F. Peden, A. Malkin, J.W. Hoard, SAE Technical Paper Series #2001-01-3513, SAE, Warrendale, PA, 2001.
[23] S.J. Schmieg, B.K. Cho, S.H. Oh, SAE Technical Paper Series #2001-01-3565, SAE, Warrendale, PA, 2001.
[24] S.E. Thomas, J.T. Shawcross, R. Gillespie, D. Raybone, A.R. Martin, SAE Technical Paper Series #2001-01-3568, SAE, Warrendale, PA, 2001.
[25] K.G. Rappe, C.L. Aardahl, C.F. Habeger, D.N. Tran, M.A. Delgado, L.-Q. Wang, P.W. Park, M.L. Balmer, SAE Technical Paper Series #2001-01-3570, SAE, Warrendale, PA, 2001.
[26] B.M. Penetrante, R.M. Brusasco, B.T. Merritt, W.J. Pitz, G.E. Vogtlin, SAE Technical Paper Series #1999-01-3687, SAE, Warrendale, PA, 1999.
[27] B.M. Penetrante, R.M. Brusasco, B.T. Merritt, W.J. Pitz, G.E. Vogtlin, SAE Technical Paper Series, Paper 1999-01-3637, SAE International, Warrendale, PA, 1999.
[28] D.N. Tran, C.L. Aardahl, K.G. Rappe, P.W. Park, C.L. Boyer, Appl. Catal. B: Environmental. MFS-2003-267 8994, 1–10.
[29] F.C. Meunier, V. Zuzaniuk, J.P. Breen, M. Olsson, J.R.H. Ross, Catal. Today 59 (2000) 287.
[30] F.C. Meunier, V. Zuzaniuk, J.P. Breen, M. Olsson, J.R.H. Ross, J. Catal. 187 (1999) 493.
[31] T. Maunula, Y. Kintaichi, M. Inaba, M. Haneda, K. Sato, H. Hamada, Appl. Catal. B 15 (1998) 291.
[32] E. Seker, J. Cavataio, E. Gulari, P. Lorpongpaiboon, S. Osuwan, Appl. Catal. A 183 (1999) 121.
[33] A. Keshavaraja, X. She, M. Flytzani-Stephanopoulos, Appl. Catal. B 27 (2000) L1.
[34] S. Sumiya, M. Saito, M. Furuyama, N. Takezawa, K. Yoshida, React. Kinet. Catal. Lett. 64 (1998) 239.
[35] K. Shimizu, A. Satsuma, T. Hattori, Appl. Catal. B 16 (1998) 319.
[36] K.A. Bethke, H.H. Kung, J. Catal. 181 (1997) 93.
[37] M.C. Kung, P.W. Park, D.-W. Kim, H.H. Kung, J. Catal. 181 (1999) 1.
[38] T. Maunula, Y. Kintaichi, M. Haneda, H. Hamada, Catal. Lett. 61 (1999) 121.
[39] P.W. Park, C.S. Ragle, C.L. Boyer, M.L. Balmer, M. Engelhard, D. McCready, J. Catal. 210 (2002) 97.
[40] T. Maunula, J. Ahola, H. Hamada, Appl. Catal. B 26 (2000) 173.
[41] F.C. Meunier, R. Ukropec, C. Stapleton, J.R.H. Ross, Appl. Catal. B 30 (2001) 163.
[42] K. Shimizu, J. Shibata, H. Yoshida, A. Satsuma, T. Hattori, Appl. Catal. B 30 (2001) 151.
[43] T. Chafik, S. Kameoka, Y. Ukisu, T. Miyadera, J. Mol. Catal. A 136 (1998) 203.
[44] F.C. Meunier, J.P. Breen, J.R.H. Ross, Chem. Commun. 1999 (1999) 259.
[45] V. Zuzaniuk, F.C. Meunier, J.R.H. Ross, Chem. Commun. 1999 (1999) 815.
[46] M. Sasaki, H. Hamada, Y. Kintaichi, T. Ito, Catal. Lett. 15 (1992) 297.
[47] R.A. Grinstedt, H.-W. Jen, C.N. Montreuil, M.J. Rokosz, M. Shelef, Zeolites 13 (1993) 602.
[48] R. Keiski, H. Raisanen, M. Harkonen, T. Maunula, P. Niemisto, Catal. Today 26 (1996) 85.
[49] J. Bonadies, Performance evaluation of the Delphi non-thermal plasma system under transient and steady-state conditions, in: Presentation Given at the Eighth Diesel Engine Emissions Reduction Conference, US DOE FreedomCAR and Vehicle Technologies, San Diego, CA, August 25–29, 2002.
[50] P.W. Park, H.H. Kung, D.-W. Kim, M.C. Kung, J. Catal. 184 (1999) 440.
[51] L.A. Rosenthal, D.A. Davis, IEEE Trans. Ind. Appl. I-5 (1975) 328.
[52] A.G. Panov, R. Tonkyn, S. Yoon, A. Kolwaite, S. Barlow, M.L. Balmer, NO_x reduction behavior of alumina and zeolite catalysts in combination with non-thermal plasma, in: Presentation Given at the Sixth Diesel Engine Emissions Reduction Workshop, US DOE FreedomCAR and Vehicle Technologies, San Diego, CA, August 2000.